DOI: 10.53469/jcmp.2026.08(04).36

Cervical Sagittal Alignment in Chiari Malformation type I with Basilar Invagination Type B: An Observational Study Using Upright X-Radiographs

Tao Chen, Guolian Chen, Baoting Chen, Yongzhi Xia*

Department of Neurosurgery, the First Affiliated Hospital of Chongqing Medical University, Chongqing 400016, China
Correspondence Author,

Abstract: ***Objective:*** ***Basilar invagination (BI) frequently coexists with Chiari malformation type I (CMI), yet its impact on global cervical sagittal alignment remains unclear. This study aimed to quantitatively evaluate the cervical sagittal alignment in adult CMI patients with type B BI, with a focus on subaxial curvature.*** ***Methods:*** ***One hundred and eight adult CMI patients (35 CMI patients with type B BI for CMI-BI group and 35 patients without for CMI-only group) and 53 controls were retrospectively included. Upright neutral lateral cervical radiographs were obtained. Craniocervical parameters, including the foramen magnum angle (FMA), basal angle (BA), clivus-axial angle (CXA), and horizontal visual axis angle (HVA), as well as cervical sagittal alignment parameters (C0–2, C2–7, and C0–7 angles, T1 slope, and C2–7 sagittal vertical axis (SVA)), were measured. Intergroup comparisons were performed using one-way analysis of variance or the Kruskal–Wallis test.*** ***Results:*** ***Significant intergroup differences were observed in multiple parameters. FMA and BA demonstrated a stepwise increase from controls to CMI-only patients, reaching the highest values in the CMI-BI group, whereas CXA and HVA decreased, indicating progressive craniocervical kyphosis. Upper cervical lordosis increased in both CMI groups, while lower cervical lordosis was markedly increased only in CMI-BI patients. The whole cervical lordosis increased synchronously, whereas T1 slope and C2–7 SVA remained unchanged.*** ***Conclusion:*** ***Under physiological load, CMI patients with type B BI demonstrate a compensatory alignment characterized by increased lordosis in both upper and subaxial cervical segments, despite craniocervical junction kyphosis, while maintaining the entire sagittal balance. The discovery of this compensatory mechanism underscores the importance of comprehensive preoperative evaluation and highlights the potential need to consider existing spinal alignment when performing fusion surgery.***

Keywords: Chiari malformation, Type B basilar invagination, Craniocervical biomechanics, Cervical sagittal balance, Upright lateral radiograph.

1. Introduction

Chiari malformation type I (CMI) is a one of the most common disorders of the craniovertebral junction. It is characterized by caudal herniation of the cerebellar tonsils through the foramen magnum (Figure 1). CMI patients often present with headache, neurological deficits, and syringomyelia due to disturbed cerebrospinal fluid dynamics [1]. A widely accepted etiological concept attributes the herniated tonsils to a congenitally small posterior cranial fossa, resulting in crowding at the foramen magnum and progressive cervicomedullary compression [2] [3].

Figure 1: Radiographic diagnostic criteria for Chiari malformation type I

Mid-sagittal T2-weighted magnetic resonance imaging demonstrating craniovertebral junction abnormalities. McRae's line (red) was drawn between the basion and opisthion, representing the anteroposterior diameter of the foramen magnum. The cerebellar tonsils (yellow arrow) were identified as the inferiorly displaced cerebellar tissue extending below the foramen magnum. The syrinx cavity (green arrow) was identified as a hyperintense intramedullary cavity within the cervical spinal cord.

Chiari malformation type I (CMI) was diagnosed when the cerebellar tonsils descended ≥5 mm below McRae's line.

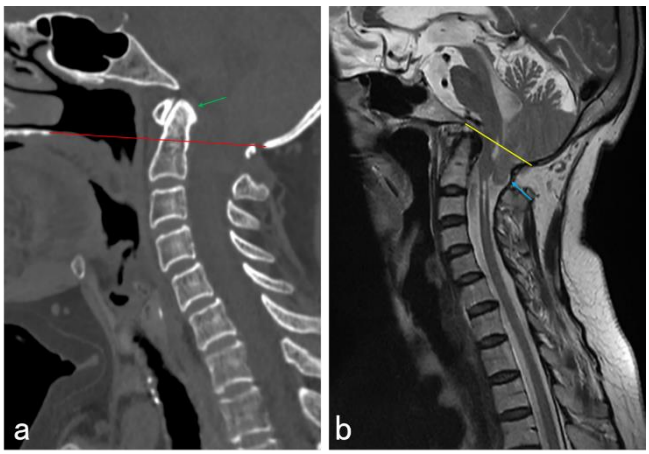

Figure 2: Radiographic diagnostic criteria for basilar invagination and Chiari malformation type I

(a) Mid-sagittal computed tomography image of the cervical spine. McGregor's line (red) was drawn from the posterior edge of the hard palate to the lowest point of the occipital curve. The green arrow indicates the tip of the odontoid

process. Basilar invagination was diagnosed when the odontoid tip projected above McGregor's line.

(b) Mid-sagittal T2-weighted magnetic resonance imaging of the craniovertebral junction. McRae's line (yellow) was drawn between the basion and opisthion. The blue arrow indicates the cerebellar tonsils. Chiari malformation type I was diagnosed when the cerebellar tonsils descended ≥5 mm below McRae's line.

Basilar invagination (BI) is a common coexisting craniovertebral anomaly in CMI. BI is defined by upward migration of the odontoid process toward or into the foramen magnum, aggravating ventral brainstem compression [4] [5]. According to the atlantoaxial stability, BI has been subclassified into type A and type B. Type B BI is characterized by odontoid invagination without radiographic evidence of altanloaxial instability [6] (Figure 2.). The CMI accompanied with type B BI presents a particular therapeutic challenge. The optimal surgical strategy remains controversial [7] [8].

Posterior fossa decompression (PFD), with or without duraplasty, is widely accepted as the main surgical treatment for symptomatic CMI. The principle of the surgery is to resolve neural compression and restore cerebrospinal fluid flow at the magnum foramen region [9] [10] [11]. In 2015, Goel et al proposed that atlantoaxial instability represents the primary pathological driver of CMI, and advocating C1–2 fixation without PFD [12]. His hypothesis, although influential, remains widely debated. Although Goel has advocated atlantoaxial fixation as a primary surgical strategy for CMI with type B BI (CMI-BI), the current literature highlights ongoing debate regarding the universal applicability of this approach. A literature review noted that Goel's proposal of a single-strategy C1–C2 fixation without decompression has been reproduced in only a limited number of series, whereas most other groups continue to combine decompression with fusion or tailor strategies based on individual anatomy and instability [13]. Importantly, there remains insufficient high-level evidence to support Goel's hypothesis, particularly in cases without clear atlantoaxial instability.

Previous morphological studies focused primarily on osseous alterations and neural compression at the posterior cranium and the craniovertebral junction. In conditions such as atlantoaxial dislocation with type A BI, compensatory hyperlordosis of the subaxial cervical spine, often referred to as a "swanneck" deformity, has been well described (Figure 3.). Itis well known to influence surgical planning [14] [15]. The craniocervical alignment will influence the postoperative neurosurgical status and have long effect on the whole cervical alignment. However, the role of the whole cervical sagittal alignment in CMI patients, particularly the subaxial cervical spine, has received limited attention.

Importantly, the minimal existing investigations relies on supine CT or MRI, which do not adequately reflect cervical alignment under physiologically weight-bearing conditions [16] [17]. Upright lateral cervical X-radiographs provide a more accurate assessment of sagittal alignment under gravitational load, which may be critical for understanding the biomechanical state of the cervical spine in this population [18] [19]. The purpose of this study was to quantitatively evaluate global cervical sagittal alignment, with a particular focus on subaxial curvature, in adult CMI patients.

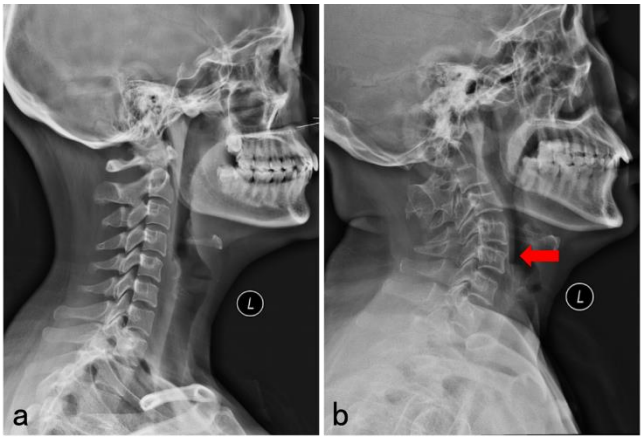

Figure 3: Swan-neck deformity in atlantoaxial dislocation

Lateral cervical radiographs demonstrating cervical sagittal alignment in a normal adult and in a patient with atlantoaxial dislocation.

(a) Neutral lateral radiograph of a normal adult showing physiological cervical lordosis.

(b) Lateral radiograph of a patient with atlantoaxial dislocation demonstrating swan-neck deformity. The red arrow indicates excessive flexion of the mid-to-lower cervical spine.

2. Methods

2.1 Study Design and Patient Population

This retrospective observational study was conducted at a single tertiary referral center. Consecutive adult patients diagnosed with symptomatic CMI who were hospitalized and treated at The First Affiliated Hospital of Chongqing Medical University between January 2015 and December 2024 were retrospectively reviewed. The study protocol was approved by the Institutional Review Board of The First Affiliated Hospital of Chongqing Medical University, and written informed consent was obtained from all participants.

Inclusion criteria were:

1) radiologically confirmed CMI, defined as cerebellar tonsillar herniation ≥5 mm below the foramen magnum on sagittal magnetic resonance imaging (MRI);

2) availability of preoperative upright neutral lateral cervical X-radiographs.

3) age ≥18 years at the time of admission.

Exclusion criteria included:

1) atlantoaxial dislocation or radiographic instability on dynamic flexion–extension radiographs.

2) occipitalization of the atlas.

3) congenital cervical segmentation anomalies (e.g., Klippel–Feil syndrome).

4) prior craniovertebral junction surgery, trauma, infection, or tumor.

5) recurrent or received any craniotomy.

6) secondary Chairi malformation

Patients were devided into three groups: the control group (healthy adults), CMI without BI (CMI-only) group, and CMI with type B BI (CMI-BI) group. BI was defined as odontoid migration >5 mm above Chamberlain's line without radiographic evidence of atlantoaxial instability, consistent with previously reported criteria.

2.2 Radiographic Parameters

All radiographic measurements were performed on standing neutral lateral cervical spine radiographs. Patients were instructed to maintain a relaxed upright posture with a horizontal gaze and to avoid voluntary neck flexion or extension during image acquisition.

Craniocervical parameters included the foramen magnum angle (FMA), defined as the angle between the McRae line and Chamberlain's line; Basal angle (BA), measured by the line between the nasion and tuberculum sellae and the line between the tuberculum sellae and basion; clivus-axial angle (CXA), defined as the angle between the clival line and the posterior axial line; Horizontal visual axis angle (HVA), defined as the angle between the extended nasion–tuberculum sellae line and the posterior axial line. [2] [20] [21] (Figure 4.)

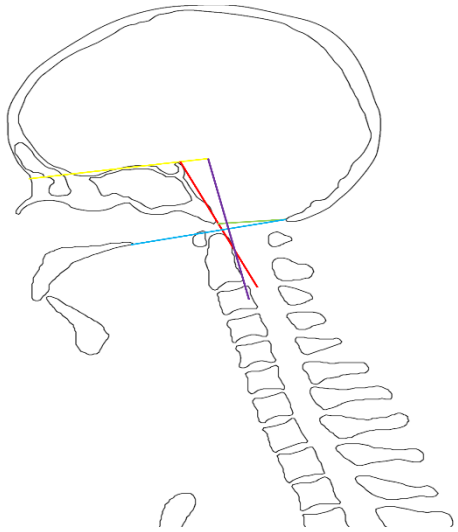

Figure 4: Craniovertebral junction parameters

The nasion–sella line (yellow) was drawn from the nasion to the center of the sella turcica. The clival line (red) was defined along the posterior surface of the clivus. McRae's line (green) was drawn between the basion and opisthion. McGregor's line (blue) was drawn from the posterior edge of the hard palate to the lowest point of the occipital curve. The posterior axial line (purple) was defined along the posterior border of the C2 vertebral body.

BA was measured between the nasion–sella line and the clival line. FMA was defined as the angle between McGregor's line and McRae's line. HVA was measured between the nasion–sella line and the posterior axial line. CXA was defined as the angle between the clival line and the posterior axial line.

Cervical sagittal alignment parameters included the C0–2 angle, C2–7 angle, C0–7 angle, T1 slope, and C2–7 sagittal vertical axis (SVA). Segmental and global cervical lordosis were measured using standard Cobb angle techniques. The T1 slope was defined as the angle between the superior endplate of T1 and the horizontal reference line, and the C2–7 SVA was measured as the horizontal distance between a vertical plumb line from the centroid of C2 and the posterosuperior corner of C7, in accordance with previously validated methodologies. [21] [22] [23] (Figure 5.)

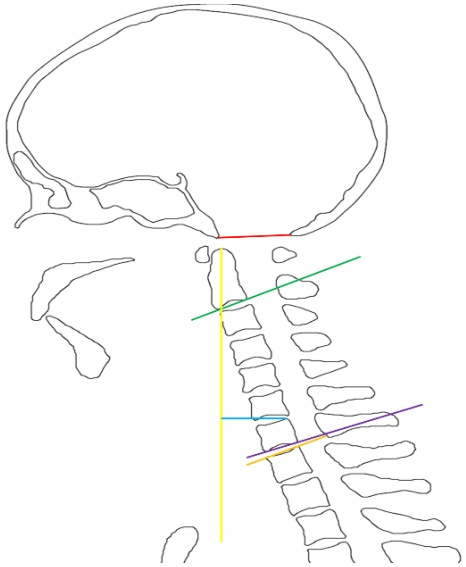

Figure 5: Cervical sagittal alignment measurements

McRae's line (red) was drawn between the basion and opisthion. The C2 vertical plumb line (yellow) was drawn from the tip of the odontoid. The inferior endplate of C2 (green) was defined along the lower border of the C2 vertebral body. The horizontal reference line (blue) was drawn perpendicular to the plumb line at the posterosuperior corner of C7. The inferior endplate of C7 (purple) was defined along the lower border of the C7 vertebral body. The superior endplate of T1 (orange) was defined along the upper border of the T1 vertebral body.

The C0–2 angle was measured between McRae's line and the inferior endplate of C2. The C0–7 angle was defined as the angle between McRae's line and the inferior endplate of C7. The C2–7 angle was measured between the inferior endplates of C2 and C7. T1 slope was defined as the angle between the superior endplate of T1 and the horizontal reference line. C2–7 sagittal vertical axis (SVA) was measured as the horizontal distance between the plumb line from the odontoid tip and the posterosuperior corner of C7.

2.3 Statistical Analysis

Statistical analyses were performed using SPSS software (version 29.0.2.0; IBM Corp., Armonk, NY, USA) and GraphPad Prism (version 10.6.0; GraphPad Software, San Diego, CA, USA). Continuous variables were assessed for normality using the Shapiro–Wilk test. Normally distributed

data are presented as mean ± standard deviation (SD) and were compared among groups using one-way analysis of variance (ANOVA). Homogeneity of variances was evaluated using Levene's test. When a significant overall difference was detected, post-hoc pairwise comparisons were conducted using Tukey's honestly significant difference (HSD) test or the Games–Howell test when the assumption of homogeneity of variance was violated. Non-normally distributed data are presented as median (interquartile range) and were analyzed using the Kruskal–Wallis test. When the Kruskal–Wallis test indicated a significant difference, post-hoc pairwise comparisons were performed using Dunn's test with adjustment for multiple comparisons. A p value < 0.05 was considered statistically significant. Categorical variables were compared using the chi-square test or Fisher's exact test.

3. Results

3.1 Demographic

A total of 161 individuals were included and divided into three groups: control group (n=53), CMI-only group (n=73), and CMI-BI group (n=35). No significant differences were observed among groups in age or sex distribution. The median age was 45 years (IQR 33.5–52) in the control group, 50 years (IQR 42.5–55) in the CMI-only group, and 49 years (IQR 40–58) in the CMI-BI group. An overall difference in age among the three groups was observed (Kruskal–Wallis test, p = 0.046). However, post hoc pairwise comparisons with multiple comparison correction revealed no statistically significant differences between any two groups (control vs. CMI-only, p = 0.06; control vs. CMI-BI, p = 0.19; CMI-only vs. CMI-BI, p > 0.99). Sex distribution did not differ significantly among the three groups (Fisher's exact test, p = 0.61). The control group included 25 males and 28 females; the CMI-only group included 28 males and 45 females; and the CMI-BI group included 15 males and 20 females. (Table. 1)

Table1: Demographic characteristics of the study population

Variables	Control (n=53)	CMI-only (n=73)	CMI-BI (n=35)	P-value
Age, years (median, IQR)	45 (33.5-52)	50 (42.5-55)	49 (30-58)	0.046 *
Male, n (%)	25 (42.7%)	28 (38.4%)	15 (42.9%)	0.61 +
Female, n (%)	28 (52.8%)	45 (61.6%)	20 (57.1%)	-

* Kruskal–Wallis test; + Fisher's exact test

Post hoc pairwise comparisons for age (Dunn's test with multiple comparison correction):
control vs. CMI-only, p = 0.06;
control vs. CMI-BI, p = 0.19;
CMI-only vs. CMI-BI, p > 0.99.

3.2 Measurement Results

3.2.1 Parametric variables

Comparisons of cervical sagittal alignment parameters are summarized in Table 2. One-way ANOVA demonstrated significant intergroup differences in HVA, C2–7 angle, and C2–7 angle (all p ≤ 0.0001).

Table 2: HVA, C2-7 Angle, C0-7 Angle, T1 Slope, C2-7 SVA using ANOVA

Group	n	HVA	C2-7 Angle	C0-7 Angle	T1 slope	C2-7 SVA
Control	53	98.32±6.83 [a]	13.28±10.25 [a]	42.13±11.15 [a]	27.82±7.62 [a]	18.71±9.07 [a]
CMI-only	73	96.48±7.85 [a]	14.02±11.67 [a]	48.48±13.83 [b]	28.24±7.54 [a]	20.5±9.89 [a]
CMI-BI	35	91.11±8.61 [b]	24.56±15.02 [b]	58.27±15.51 [c]	31.04±9.57 [a]	19.51±9.31 [a]
Statistic						
F-value		F (2, 158) =9.585	F (2, 154) = 10.97	F (2, 155) = 14.83	F (2, 151) = 1.860	F (2, 154) = 0.5298
P-value		0.0001	0.0001	<0.0001	0.1592	0.5898

*Data are presented as Mean ± Standard Deviation (SD). Significant overall differences were determined by one-way analysis of variance (ANOVA). Tukey's honestly significant difference (HSD) post hoc test was used for pairwise comparisons. Within each column, different superscript letters (a, b, c) denote statistically significant differences at P < 0.05. Groups sharing a common letter are not significantly different.

HVA was significantly greater in the CMI-BI group compared with both the control and CMI-only groups (both p < 0.005), whereas no difference was observed between the control and CMI-only groups.

The C0–7 angle demonstrated a stepwise increase from controls to CMI-only patients and was highest in the CMI-BI group (overall p < 0.0001), with significant differences confirmed across all pairwise comparisons (all p < 0.05).

Similarly, the C2–7 angle differed significantly among groups (overall p = 0.0001), with higher values observed in the CMI-BI group compared with both the control and CMI-only groups (both p = 0.0001), while no significant difference was identified between the latter two groups.

In contrast, T1 slope and C2–7 SVA did not differ significantly among the three groups.

3.2.2 Non-parametric variables

For non-normally distributed parameters (Table. 3), the Kruskal–Wallis test demonstrated significant overall differences in FMA, basal angle, CXA, and C0–2 angle (all p < 0.0001).

Table 3: FMA, BA, CXA, C0-2 Angle using Kruskal-Walli's test

Group	n	FMA	BA	CXA	C0-2 Angle
Control	53	13.2 (9.95-16.45) [a]	128.4 (125.3-131.9) [a]	158.5 (151.5-163.8) [a]	30.1 (22.15-36.15) [a]
CMI-only	73	16.5 (13-19.2) [b]	132.6 (128.5-137.2) [b]	153.2 (148.5-157.2) [b]	34.6 (28.25-39.8) [b]
CMI-BI	35	22.5 (19.6-28.3) [c]	136.5 (134-139.6) [c]	149.1 (139.3-154.4) [b]	33.2 (27.7-40.5) [a, b]
Statistic					
H-value		H (2) =41.16	H (2) =36.17	H (2) =25.45	H (2) =12.06
P-value		<0.0001	<0.0001	<0.0001	0.0024

* Data are presented as Median [Interquartile Range, IQR]. The Kruskal-Walli's test was used for overall comparisons. Within each column, different superscript letters (a, b, c) indicate statistically significant differences between groups at P < 0.05.

FMA and BA both exhibited a progressive increase from controls to CMI-only and further to CMI-BI. Post hoc Dunn's testing confirmed significant differences across all pairwise comparisons for both parameters (all p < 0.05).

CXA showed significant group-dependent variation, with

smaller values observed in both CMI groups compared with controls (both $p < 0.01$). Additionally, a modest but statistically significant reduction was identified in the CMI-BI group compared with the CMI-only group ($p < 0.05$).

For the C0–2 angle, a significant difference was observed only between the control and CMI-only groups ($p < 0.01$), whereas no significant differences were detected between the control and CMI-BI groups or between the two CMI groups.

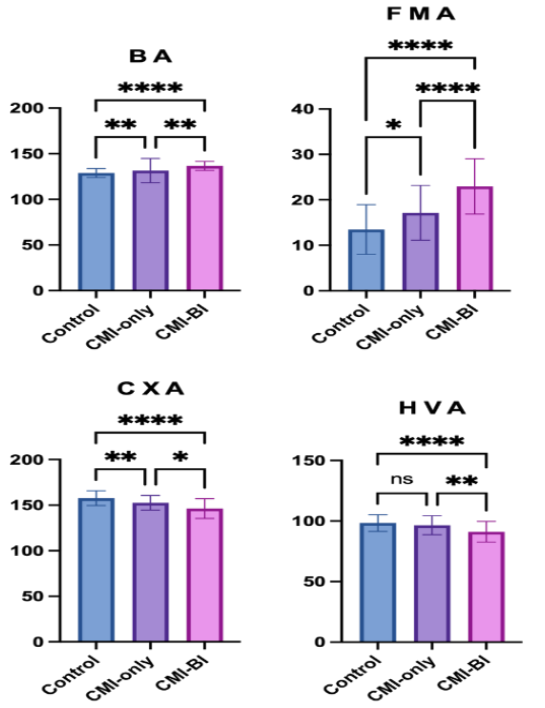

Figure 6: Comparison of craniovertebral junction measurements among the three groups

*p < 0.05, **p < 0.01, ***p < 0.001, ****p < 0.0001

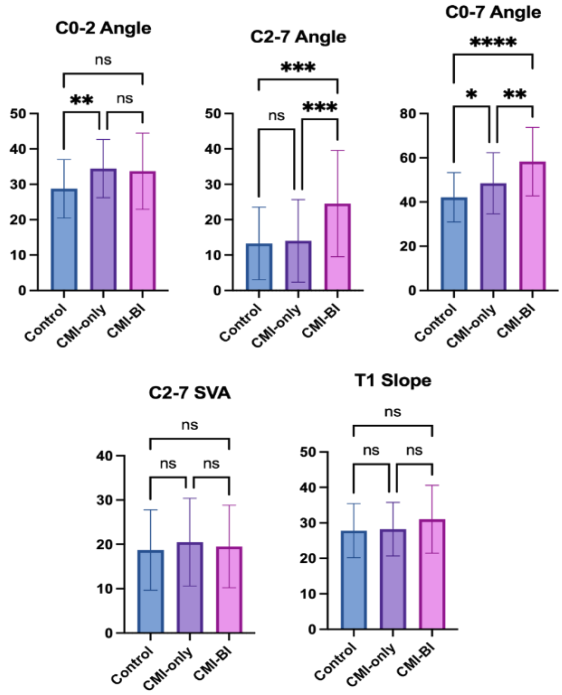

Figure 7: Comparison of cervical sagittal alignment measurements among the three groups

*p < 0.05, **p < 0.01, ***p < 0.001, ****p < 0.0001

4. Disscution

Taken together, the present radiographic analyses reveal a coherent pattern of cervical sagittal alignment changes across the spectrum of CMI with and without type B basilar invagination. The observed alterations involve coordinated changes at the craniocervical junction and cervical spine rather than isolated or random angular deviations. This kind of distinct regional differences and preserves global sagittal balance. These findings provide an anatomical and biomechanical context for interpreting the compensatory nature of cervical alignment in this patient population and form the basis for the subsequent discussion of underlying mechanisms and clinical implications.

Alterations in CVJ morphology, including BA enlargement and CXA reduction, have long been recognized as radiographic markers of ventral brainstem angulation and cranial flexion in craniovertebral junction disorders [20]. In the present cohort, the progressive reduction in CXA and HVA in the CMI-only and CMI-BI patients suggests increasing craniocervical kyphosis and anterior cranial inclination. From a biomechanical perspective, such changes would be expected to shift the head's center of gravity anteriorly, thereby necessitating adaptive responses in the cervical spine to preserve horizontal gaze and functional balance. We observed reciprocal increases in cervical lordosis, supporting the concept that the cervical spine functions as an integrated compensatory unit rather than as isolated segments.

It was reported that cervical curvature adjustments are tightly coupled to head orientation and visual axis requirements. It was an adaptive mechanism to preserve horizontal gaze in the presence of craniocervical deformity [24]. In line with this concept, CMI-BI patients demonstrated a characteristic pattern of increased upper and subaxial cervical lordosis accompanied by craniovertebral junction osseous alterations. Importantly, these regional angular changes occurred without significant alterations in global cervical balance parameters, including T1 slope and C2–7 sagittal vertical axis, as assessed on upright neutral lateral radiographs. Such an alignment pattern indicates that the observed cervical lordotic changes represent a physiological compensatory response to progressive CVJ kyphotic morphology, which allows maintenance of horizontal gaze under upright axial loading conditions.

Our findings of increased lordosis in both the upper and subaxial cervical spine in CMI- BI patients warrant comparison with existing literature. It was reported that a different pattern in BI patients: decreased upper cervical lordosis with compensatory increase in lower cervical lordosis by Lin et al. and Zhou et al. [22] [23]. This apparent discrepancy may be explained by critical differences in study populations. Neither study stratified BI according to Goel's classification, and their cohorts likely included mixed type A and type B cases potentially driving the observed reduction in upper cervical lordosis. In contrast, our study specifically focused on a homogeneous cohort of CMI-BI, explicitly excluding atlantoaxial instability. The increased upper cervical lordosis we observed may reflect a distinct compensatory mechanism arising from skull base deformation intrinsic to type B BI, rather than a response to radiographic

instability.

It was reported that subaxial cervical alignment parameters, including C2 tilt and C7 slope, were not significantly altered in patients with Chiari malformation, suggesting that cervical curvature changes largely remain within a compensatory range [25]. Our findings in the CMI-only group are consistent with this observation. In contrast, the presence of type B BI in our cohort was associated with significant alterations in subaxial cervical lordosis, indicating that BI may represent a critical modifier of cervical compensatory mechanisms.

Our findings are consistent with a MRI-based-study specifically examining patients with type B BI, which demonstrated significantly increased cervical lordosis — particularly within the C2–C6 and C2–C4 segments [17]. The authors suggested that skull base deformation and clival hypoplasia intrinsic to type B BI may directly drive cervical hyperlordosis. This study relied on supine MRI and therefore may not have fully accounted for the effects of physiological loading or neck posture during image acquisition. Moreover, our consistent results of increased cervical lordosis using upright X-radiographs reinforces the notion that cervical curvature changes in type B BI are structural and compensatory in nature.

Notably, despite regional angular changes, global cervical sagittal balance was preserved in our cohort, as evidenced by the absence of significant intergroup differences in T1 slope and C2-7 SVA. This finding contrasts with reports in patients with atlantoaxial dislocation, in whom exaggerated subaxial hyperlordosis is frequently accompanied by increased C2–7 SVA and sagittal decompensation [14]. The discrepancy likely reflects biomechanical differences between reducible atlantoaxial instability and type B BI without radiographic instability. In the latter, compensatory mechanisms appear to remain effective and well distributed across cervical segments, allowing maintenance of overall sagittal equilibrium.

The use of upright radiographs represents a critical methodological advantage of the present study. Previous investigations based on supine CT or MRI may underestimate cervical lordosis and fail to capture load-dependent compensatory mechanisms. Upright imaging more accurately reflects the sustained gravitational forces acting on the cervical spine during daily activities and provides a more realistic assessment of sagittal alignment [18] [19].

Overall, the presence of type B BI may be a key factor driving alterations in subaxial cervical lordosis. CMI patients with concomitant type B BI demonstrated increased curvature in the lower cervical segments compared with CMI-only patients, suggesting that the compensatory mechanisms extend beyond the upper cervical spine. Importantly, despite these regional changes, global cervical sagittal balance parameters, including T1 slope and C2–7 SVA, remained largely preserved. This indicates that while type B BI may influence subaxial alignment, the cervical spine functions as an integrated unit to maintain an effective compensatory strategy and preserve overall sagittal equilibrium.

The study has important implications for surgical decision-making in CMI patients with or without type B BI. While atlantoaxial fixation has been advocated by some authors based on the hypothesis that occult instability underlies both CMI and BI [12], contemporary consensus statements emphasize individualized treatment strategies and recommend fusion primarily for cases with demonstrable instability or irreducible deformity [26]. Our findings suggest that CMI patients with type B BI maintain an effective and compensated cervical sagittal alignment. Any surgical interventions that may alter CVJ alignment without consideration of this existing compensation may risk iatrogenic sagittal imbalance. Therefore, comprehensive preoperative assessment should extend beyond the CVJ to global cervical sagittal alignment parameters, particularly when the fixation and fusion surgery is considered.

5. Conclusion

In summary, this study identifies a distinct cervical sagittal alignment profile in CMI patients with type B BI. Using upright lateral cervical X-radiographs, which reflect physiological spinal loading, compensatory increases in both upper and subaxial cervical lordosis were observed, while the whole sagittal cervical balance was maintained. These adaptations may be tentatively interpreted as a biomechanical response to maintain a horizontal gaze in the setting of increased craniovertebral junction kyphosis.

These findings highlight the importance of evaluating the entire cervical spine, not solely the craniovertebral junction, in the preoperative assessment of CMI patients. Consideration of such compensatory alignment may help refine surgical decision-making, particularly when weighting PFD against atlantoaxial or craniocervical fixation, and may contribute to reconciling differing surgical paradigms.

Ethics Approval

This retrospective study was approved by the Ethics Committee of the First Affiliated Hospital of Chongqing Medical University. Due to the retrospective nature of the study and the use of anonymized imaging data, the requirement for written informed consent was waived. All procedures were conducted in accordance with the Declaration of Helsinki and relevant guidelines and regulations. The science and health joint project of Chongqing City [No. 2025MSM172] provided financial support.

Conflict of Interest Statement

The authors declare that the article content was composed in the absence of any commercial or financial relationships that could be construed as a potential conflict of interest.

Acknowledgement

This work was supported by the Science and Health Joint Project of Chongqing City [No. 2025MSXM172].

References

[1] Milhorat TH, Chou MW, Trinidad EM, et al. Chiari I malformation redefined: clinical and radiographic findings for 364 symptomatic patients. Neurosurgery. 1999; 44(5):1005-1017.doi:10.1097/00006123-199905000-00042

[2] Xia Y, Xia H, Tang W, Wang S, Yan Y. Morphometric and volumetric analysis of the posterior cranial fossa in adult Chiari malformation type I with and without group B basilar invagination. J Integr Neurosci. 2022;21(2):70. doi:10.31083/j.jin2102070

[3] Wang S, Huang Z, Xu R, et al. Chiari Malformations Type I without Basilar Invagination in Adults: Morphometric and Volumetric Analysis. World Neurosurg. 2020; 143: e640-e647. doi:10.1016/j.wneu.2020.08.048

[4] Brito JNPO, Santos BAD, Nascimento IF, Martins LA, Tavares CB. Basilar invagination associated with chiari malformation type I: A literature review. Clinics (Sao Paulo). 2019;74:e653. doi:10.6061/clinics/2019/e653

[5] Saunders WW. Basilar Impression: The Position of the Normal Odontoid. Radiology. 1943/12/01 1943; 41(6): 589-590. doi:10.1148/41.6.589

[6] Goel A. Basilar invagination, Chiari malformation, syringomyelia: a review. Neurol India. 2009; 57(3): 235-246. doi:10.4103/0028-3886.53260

[7] Goel A, Sathe P, Shah A. Atlantoaxial Fixation for Basilar Invagination without Obvious Atlantoaxial Instability (Group B Basilar Invagination): Outcome Analysis of 63 Surgically Treated Cases. World Neurosurg. 2017; 99: 164-170. doi:10.1016/j.wneu.2016.11.093

[8] Joaquim AF, Neto ER, Pinheiro LCP, et al. Surgical Treatment of Basilar Invagination without Evident Atlantoaxial Instability (Type B) - A Systematic Review. Neurol India. 2025; 73(3): 423-428. doi:10.4103 / neurol-india. Neurol-India-D-24-00457

[9] Klekamp J. Surgical treatment of Chiari I malformation--analysis of intraoperative findings, complications, and outcome for 371 foramen magnum decompressions. Neurosurgery. 2012;71(2):365-380. doi:10.1227/NEU.0b013e31825c3426

[10] Lin W, Duan G, Xie J, Shao J, Wang Z, Jiao B. Comparison of Results Between Posterior Fossa Decompression with and without Duraplasty for the Surgical Treatment of Chiari Malformation Type I: A Systematic Review and Meta-Analysis. World Neurosurg. 2018; 110: 460-474.e5. doi:10.1016/j.wneu.2017.10.161

[11] Osborne-Grinter M, Arora M, Kaliaperumal C, Gallo P. Posterior Fossa Decompression and Duraplasty with and without Arachnoid Preservation for the Treatment of Adult Chiari Malformation Type 1: A Systematic Review and Meta-Analysis. World Neurosurg. 2021; 151: e579-e598. doi:10.1016/j.wneu.2021.04.082

[12] Goel A. Is atlantoaxial instability the cause of Chiari malformation? Outcome analysis of 65 patients treated by atlantoaxial fixation. J Neurosurg Spine. 2015;22(2):116-127. doi:10.3171/2014.10.SPINE14176

[13] Wagner A, Grassner L, Kögl N, et al. Chiari malformation type I and basilar invagination originating from atlantoaxial instability: a literature review and critical analysis. Acta Neurochir (Wien). 2020; 162(7): 1553-1563.doi:10.1007/s00701-020-04429-z

[14] Wang S, Passias PG, Cui L, et al. Does atlantoaxial dislocation influence the subaxial cervical spine?. Eur Spine J. 2013; 22(7): 1603-1607. doi:10.1007/s00586-013-2742-4

[15] Passias PG, Wang S, Zhao D, Wang S, Kozanek M, Wang C. The reversibility of swan neck deformity in chronic atlantoaxial dislocations. Spine (Phila Pa 1976). 2013;38(7):E379-E385.doi:10.1097/BRS.0b013e31828625e4

[16] Karabağ H, İplikçioğlu AC. Evaluation of cervical sagittal parameters on supine magnetic resonance imaging in patients with Chiari I malformation without syringomyelia. Neurochirurgie. 2022;68(5):504-509. doi:10.1016/j.neuchi.2022.04.007

[17] Silva KMS, Silva LM, Nascimento JJC, et al. Effect of the Basilar Invagination (Type B) on Cervical Spine: A Case-control Study with MRI. World Neurosurg. 2024;191:e373-e380. doi:10.1016/j.wneu.2024.08.133

[18] Sevin IE, Bozdag S, Erisken E, Sucu HK. Comparison of Radiography with Computed Tomography and Magnetic Resonance Imaging in the Measurement of Cervical Lordosis. Medicina (Kaunas). 2025;61(9):1654. Published 2025 Sep 11. doi:10.3390/medicina61091654

[19] Boudreau C, Carrondo Cottin S, Ruel-Laliberté J, Mercier D, Gélinas-Phaneuf N, Paquet J. Correlation of supine MRI and standing radiographs for cervical sagittal balance in myelopathy patients: a cross-sectional study. Eur Spine J. 2021;30(6):1521-1528. doi:10.1007/s00586-021-06833-0

[20] Smoker WR. Craniovertebral junction: normal anatomy, craniometry, and congenital anomalies. Radiographics. 1994;14(2):255-277.doi:10.1148/radiographics.14.2.8190952

[21] Huang H, Sheng M, Zeng G, Sun C, Li R. Establish a new parameter "horizontal view-axial angle" and explore its role in the treatment of atlantoaxial instability diseases. Front Surg. 2023;9:947462. Published 2023 Jan 6. doi:10.3389/fsurg.2022.947462

[22] Lin JY, Bao MG, Lin SY, Liu JH, Liu Q, Li RY, Huang ZC, Zhu QA, Zhang ZM, Ji W. Cervical Alignment of Patients with Basilar Invagination: A Radiological Study. Orthop Surg. 2022 Mar; 14(3): 566-576. doi: 10.1111/os.13212. Epub 2022 Feb 13. PMID: 35156312; PMCID: PMC8926990.

[23] Zhou Y, Hou J, Xiao R, Zheng J, Zou X, Zhu Y, Yao L, Chen J, Ma X, Yang J. Cervical Sagittal Alignment in Patients With Basilar Invagination. Spine (Phila Pa 1976). 2022 Nov 1; 47(21): 1515-1524. doi: 10.1097/BRS.0000000000004423. Epub 2022 Jul 15. PMID: 35867616.

[24] Cui S, Wang X, Li K, et al. Introducing Angle B: A Novel Quantitative Approach for Sagittal Alignment Reduction in Atlanto-Axial Dislocation Surgery. Ther Clin Risk Manag. 2024;20:789-797. Published 2024 Nov 26. doi:10.2147/TCRM.S483075

[25] Karadeniz R, Dağlar Z, Çağıl E, et al. The head position and cervical alignment in patients with Chiari malformation: A retrospective case-control study. J Craniovertebr Junction Spine. 2024;15(4):460-466. doi:10.4103/jcvjs.jcvjs_164_24

[26] Klekamp J, Alves OL, Zileli M, et al. Incidence and Management of Basilar Invagination With Associated Chiari I Malformation: WFNS Spine Committee Recommendations. Spine (Phila Pa 1976). 2025; 50(11): 786-791.doi:10.1097/BRS.0000000000005293